



## Structural Response Diagram Approach for Evaluation of Thermal Striping Phenomenon

Naoto Kasahara<sup>1)</sup>, Apisara Yacumpai<sup>1)</sup> and Hideki Takasho<sup>2)</sup>

1) *Japan Nuclear Cycle Development Institute, Japan*

2) *Joyo Industries Ltd., Japan*

### Abstract

Based on investigations of frequency response characteristics of structures to fluid temperature fluctuation and its mechanism, a structural response diagram was derived, which can predict stress amplitude of structures from temperature amplitude and frequency of fluids. Furthermore, this diagram was generalized to a non-dimensional structural response diagram by introducing non-dimensional parameters such as Biot number, non-dimensional frequency, and non-dimensional stress. This diagram appears to be able to rationally evaluate thermal stress caused by thermal striping and also to give information on frequency range to which structural integrity is sensitive.

### 1. Introduction

At an incomplete mixing area of high and low temperature fluids near the surface of structures, temperature fluctuation of fluid gives thermal fatigue damage to the wall structures. This coupled thermohydraulic and thermomechanical phenomenon is called thermal striping, which has so complex mechanism and sometimes causes crack initiation on the structural surfaces that sodium mock-up tests are usually required to confirm structural integrity of components against this phenomenon.

Recent investigation on thermal striping has revealed that amplitude of temperature fluctuation was attenuated during a series of heat transfer process from fluids to structures by ①turbulent mixing, ② molecular diffusion, ③non-stationary heat transfer, and ④thermal unloading as in Fig.1[1]. When taking these attenuation factors into consideration, rational evaluation on thermal striping will be realized[2]. However, the attenuation process is a thermal coupling problem between fluids and structures and has a sensitive characteristics to frequencies of temperature fluctuations. Therefore, time history analyses using coupled thermohydraulic and thermomechanical models are generally required to consider above factors. Realizing that coupled analysis methods are too time consuming to be used as screening methods for design, the authors commenced a development of the structural response diagram approach. Through investigation of frequency response characteristics of structures and their mechanisms, the non-dimensional structural response diagram (NSRD) is derived considering attenuation factors ③ and ④ in Fig.1. The use of the NSRD will enable rapid and rational evaluation of thermal striping. Another advantage of this approach is feedback from structural characteristics to thermal hydraulic analysis(Fig.2). For detailed evaluation taking above four kinds of attenuation factors into account, coupled thermohydraulic and thermomechanical models are required. To make rational and accurate analysis models, NSRD can give useful information such as frequency range to which structural integrity is sensitive.

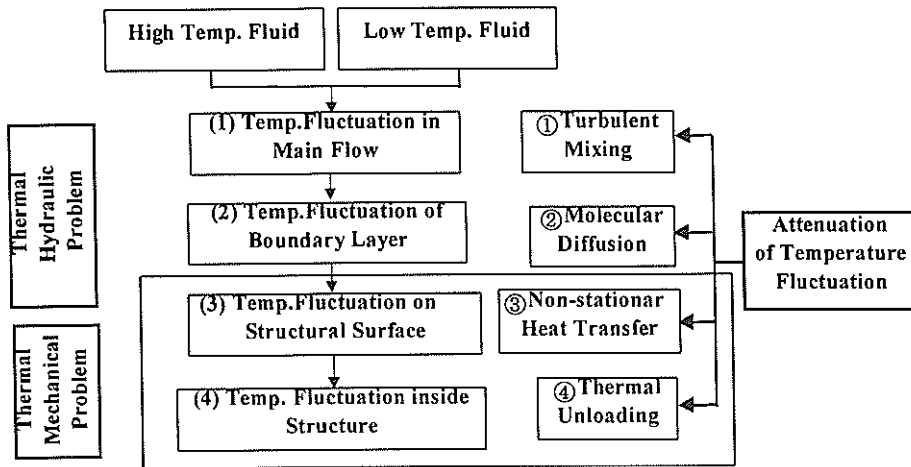


Fig.1 Attenuation factors of temperature fluctuation amplitude during a series of heat transfer process from fluid to structures

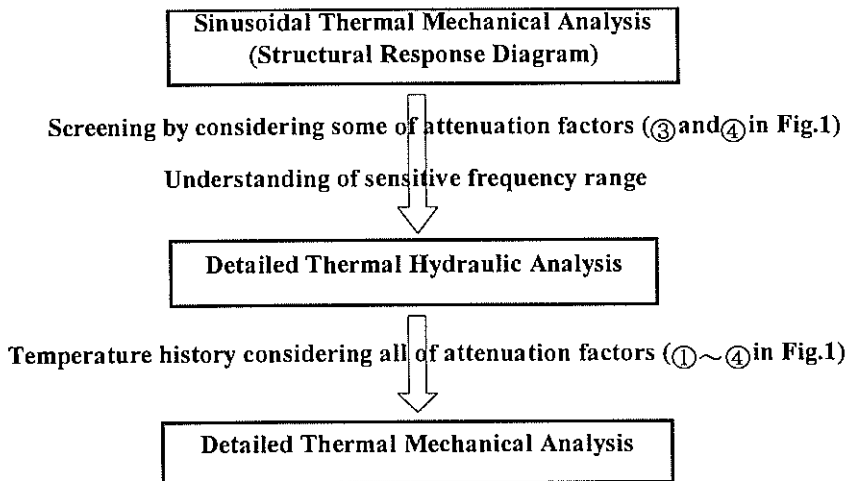


Fig.2 Concept of structural response diagram approach

## 2. Frequency response characteristics of a pipe wall

In order to grasp sensitivity of structural responses to frequency of fluid temperature fluctuations, a pipe wall due to sinusoidal fluid temperature fluctuation with various frequencies was analyzed by the finite element analysis code FINAS[3]. A pipe wall model with thermal boundary condition is as shown in Fig.3, where wall thickness  $L$  is 7 mm, inner diameter is 494mm, and material is Type 304 stainless steel. The inner surface of the pipe is subjected to sinusoidal temperature fluctuation of fluid with constant amplitude  $\Delta T_f$  as  $90^\circ\text{C}$  (maximum temperature is  $430^\circ\text{C}$  and minimum temperature is  $340^\circ\text{C}$ ) and the outer surface is kept adiabatic. This study assumed constant heat-transfer coefficient  $h$  whose value was  $14500\text{kcal/m}^2\text{h}^\circ\text{C}$ . Stress amplitudes caused by sinusoidal temperature fluctuation of fluid with frequencies of 0.01 Hz, 0.03 Hz, 0.07 Hz, 0.0846 Hz, 0.1 Hz, 1.0 Hz and 10 Hz were calculated and were summarized to a structural response diagram (SRD) as in Fig.4.

A noteworthy point from this figure is that stress amplitude varies according to frequency and takes its maximum value 243MPa at the particular frequency 0.0846Hz, even though amplitude of temperature fluctuation is constant. It means that stress amplitude is always less than 243MPa against random fluctuations. When frequency range is limited, the maximum value of stress amplitude can be evaluated according to the frequency range. Thermal striping evaluation methods have conventionally adopted the next equation to calculate thermal stress range  $\Delta \sigma$  from fluid temperature amplitude  $\Delta T$ [4].

$$\Delta \sigma = \frac{E\alpha}{1-\nu} \Delta T, \tag{1}$$

where E is Young’s modulus,  $\alpha$  is thermal expansion ratio, and  $\nu$  is Poisson’s ratio.

When substituting 90 K to  $\Delta T$  of Eq.(1), thermal stress range  $\Delta \sigma$  is evaluated as 353MPa. From this fact, the SRD appears to be a rational evaluation tool than Eq.(1).

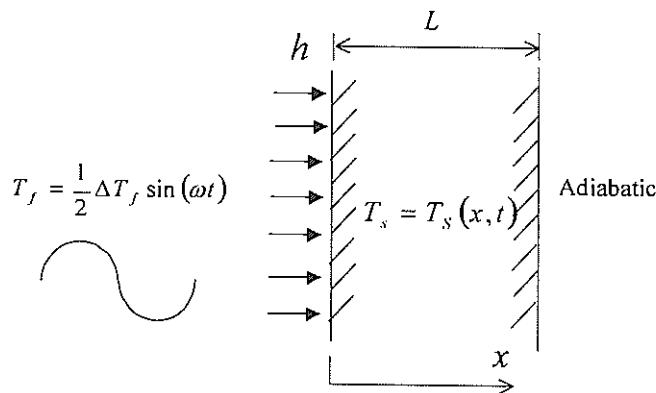


Fig.3 A pipe wall model subjected to sinusoidal temperature fluctuation

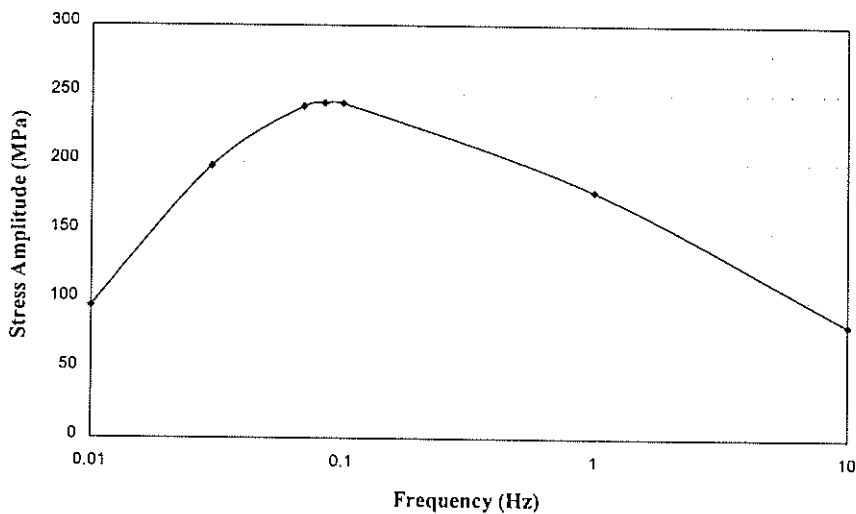


Fig.4 Stress amplitude induced by sinusoidal temperature fluctuation

### 3. Mechanism of structural responses to sinusoidal temperature fluctuations

In order to understand mechanism of structural responses to sinusoidal temperature fluctuations, theoretical approach is adopted to solve thermal and mechanical responses of a pipe wall due to sinusoidal temperature fluctuation shown in Fig.3. For thermal transient problems, plates with the same wall thickness are fairly good approximation of thin pipes, when diameter is more than ten times than wall thickness[5]. To simplify the formulation, let us introduce another approximation, that is, we assume we can use the theoretical distribution in a semi-infinite solid to a fluid temperature fluctuation. Accuracy of this approximation will be examined in the later. For a semi-infinite solid shown in Fig.5, the 1-D heat conduction equation is

$$\frac{\partial T}{\partial t} = \frac{\lambda}{\rho c} \frac{\partial^2 T}{\partial x^2} \quad (2)$$

where  $T$  is temperature,  $t$  is time,  $\lambda$  is thermal conductivity,  $c$  is specific heat, and  $\rho$  is density.

When fluid temperature fluctuates in sinusoidal way and is transferred to the surface of the semi-infinite solid with a constant heat-transfer coefficient  $h$  as in Fig.5, boundary condition is

$$-\lambda \left. \frac{\partial T}{\partial x} \right|_{x=0} = h(T|_{x=0} - T_f), \quad T_f = \frac{1}{2} \Delta T_f \sin(\omega t) \quad (3)$$

where  $h$  is the heat-transfer coefficient,  $\Delta T_f$  is the amplitude of fluid temperature fluctuation, and  $\omega$  is circular frequency.

Temperature of structures  $T_s$  can be derived as a function of distance  $x$  from the surface and time  $t$ .

$$T_s = T_s(x, t) = \frac{1}{2} \Delta T_s e^{-kx} \sin(\omega t - kx - \varepsilon), \quad (4)$$

where amplitude of structural temperature fluctuation  $\Delta T_s = \frac{\Delta T_f h^*}{\sqrt{(h^* + k)^2 + k^2}}$ ,

$$k = \sqrt{\frac{\omega}{2a}}, \quad a = \frac{\lambda}{c\rho}, \quad h^* = \frac{h}{\lambda}, \quad \text{and} \quad \varepsilon = \tan^{-1} \left[ \frac{k}{(h^* + k)} \right].$$

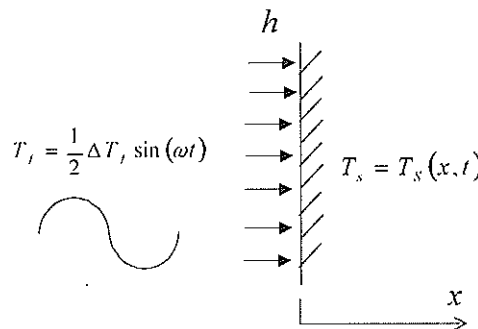


Fig.5 Thermal response of a semi-infinite solid to sinusoidal temperature fluctuation of fluid

When substituting the material properties of Type304SS, fluid temperature amplitude  $251^\circ\text{C}$  (Maximum Temperature: $381^\circ\text{C}$ , Minimum Temperature: $130^\circ\text{C}$ ), and heat transfer coefficient  $8.8517 \times 10^{-6} \text{ kcal/mm}^2\text{sec}^\circ\text{C}$  into Eq.(4), temperature profiles in the semi-infinite solid due to sinusoidal temperature fluctuation with various frequencies can be calculated as in Fig.6. An

important point from these results is that temperature amplitude is reduced monotonously when frequency becomes high. This trend can be explained by Eq.(4) where the term of amplitude of structural temperature fluctuation  $\Delta T_s$ , contains frequency in the denominator. Its physical meaning is considered as attenuation factors by non-stationary heat transfer. By using temperature distribution derived from Eq.(4), induced thermal stress distribution  $\sigma(x,t)$  can be quantitatively evaluated by thermal elastic theory as

$$\begin{aligned} \sigma(x,t) &= \frac{E\alpha}{1-\nu} \left\{ T_s(x,t) - \frac{1}{L} \int_0^L T_s(x,t) dx \right\} \\ &= \frac{E\alpha\Delta T_s}{2(1-\nu)} \left\{ e^{-kx} \sin(\alpha t - kx - \varepsilon) - \frac{1}{L} \int_0^L e^{-kx} \sin(\alpha t - kx - \varepsilon) dx \right\} \\ &= \frac{E\alpha\Delta T_s}{2(1-\nu)} \left[ e^{-kx} \sin(\alpha t - kx - \varepsilon) + \frac{1}{\sqrt{2kL}} \left\{ e^{-kL} \sin\left(\alpha t - kL - \varepsilon - \frac{\pi}{4}\right) - \sin\left(\alpha t - \varepsilon - \frac{\pi}{4}\right) \right\} \right]. \end{aligned} \quad (5)$$

From Eq.(5), stress amplitude is understood to be a function of heat convection, frequency, wall thickness, thermal conductivity, specific heat, density, Young's modulus, and thermal expansion ratio.

Eq.(5) also explains that thermal stress is caused by temperature deviation of evaluation points from average temperature of wall thickness. In the case of low frequency of fluctuation, average temperature can follow temperature change of evaluation points because of heat conduction in the wall thickness, consequently thermal stress is mitigated. It is considered to be the attenuation factor from thermal unloading in Fig.1.

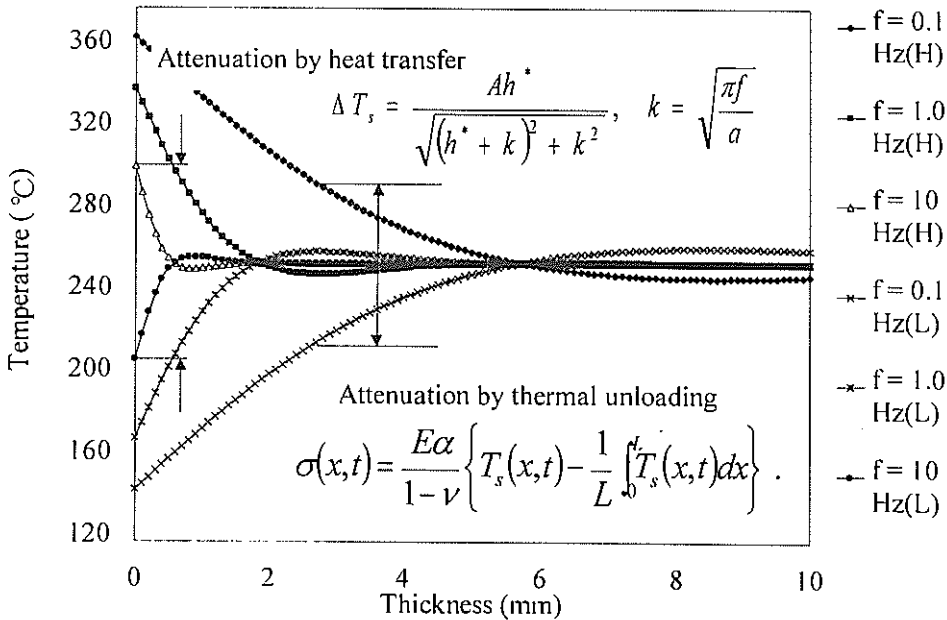


Fig.6 Temperature profile in a semi-infinite solid due to sinusoidal temperature fluctuation

#### 4. Non-dimensional structural response diagram (NSRD)

Based on Eq.(5), more general equations and diagrams will be derived for adoption to design use, by introduction of the following non-dimensional parameters: , i.e.

$Bi = \frac{hL}{\lambda}$  : Biot number,  $t^* = \frac{ta}{L^2}$  : Fourier number,  $f^* = \frac{fL^2}{a}$  : non-dimensional frequency defined

in this study, and  $\sigma^* = \sigma|_{x=0} / \frac{E\alpha\Delta T_f}{1-\nu}$  : non-dimensional thermal stress defined by the ratio of actual thermal stress to ideal thermal stress converted from 100% of fluid temperature amplitude.

By substituting above non-dimensional parameters into Eq.(5) and neglecting the term of phase delay which has no influence on stress amplitude, non-dimensional stress at the inner surface ( $x=0$ ) can be described as

$$\sigma^* = \frac{1}{2} H(B_i, f^*) \Lambda(f^*, t^*) \tag{6}$$

$$\text{where } H(B_i, f^*) = \frac{B_i}{\sqrt{(B_i + \sqrt{\pi f^*})^2 + \pi f^*}} \tag{7}$$

which is attenuation factor by non-stationary heat transfer, and

$$\Lambda(f^*, t^*) = \sin(2\pi f^* t^*) + \frac{1}{\sqrt{2\pi f^*}} \left\{ e^{-\sqrt{\pi f^*}} \sin\left(2\pi f^* t^* - \sqrt{\pi f^*} - \frac{\pi}{4}\right) - \sin\left(2\pi f^* t^* - \frac{\pi}{4}\right) \right\} \tag{8}$$

which is attenuation factor by thermal unloading.

By using Eqns.(6) through (8), relationship between amplitude of non-dimensional thermal stress  $\Delta\sigma^*$  and non-dimensional frequency  $f^*$  were calculated for the different Biot number  $B_i$  as in Fig.7, which is named the non-dimensional structural response diagram (NSRD).

Here, defining of the heat-transfer coefficient is difficult for the thermal stripping problem since this value is actually non-stationary during fluctuation. Therefore, R&Ds for a heat-transfer problem between fluid and structure under thermal stripping phenomena are required to determine rational Biot number for the NSRD.

$$\sigma^* = \frac{1}{2} H(B_i, f^*) \Lambda(f^*, t^*) \quad H(B_i, f^*) = \frac{B_i}{\sqrt{(B_i + \sqrt{\pi f^*})^2 + \pi f^*}} \quad \Lambda(f^*, t^*) = \sin(2\pi f^* t^*) + \frac{1}{\sqrt{2\pi f^*}} \left\{ e^{-\sqrt{\pi f^*}} \sin\left(2\pi f^* t^* - \sqrt{\pi f^*} - \frac{\pi}{4}\right) - \sin\left(2\pi f^* t^* - \frac{\pi}{4}\right) \right\}$$

③ Non-stationary Heat Convection
④ Thermal Unloading

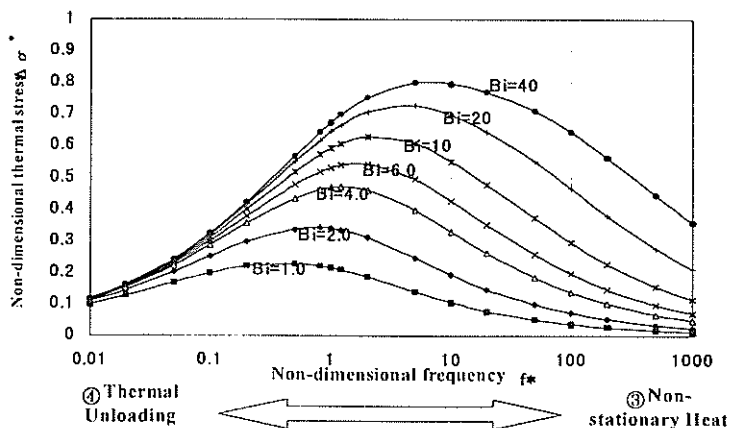


Fig.7 Non-dimensional Structural Response Diagram (NSRD)

**5. Verification of non-dimensional structural response diagram**

Accuracy of the derived NSRD under assumption of 1-D heat conduction of a semi-infinite solid was verified through comparison with F.E. calculated results. Structural responses of the pipe wall subjected to sinusoidal fluid temperature were calculated by FINAS code and were plotted in the NSRD. Analysis conditions were almost the same as the chapter two and a different point from the original problem is wall thickness, which was changed to 1.049553 mm, 6.297319 mm, and 41.98213 mm for control of Biot number. The same problem was evaluated by Eqns.(6)-(8), which was named as a theoretical NSRD to distinguish from numerical one, and was over plotted into Fig.8. What are evident from Fig.8 are as follows. Numerical NSRD is equivalent to theoretical NSRD when non-dimensional frequency is high, since temperature of the inner surface calculated by both methods was the same and average temperature of the wall was constantly the intermediate value of the maximum and the minimum temperature of temperature fluctuation. On the other hand, stresses of theoretical NSRD are larger than ones of Numerical NSRD in low frequency region, because the amplitude of theoretically calculated average temperature of the wall was larger than numerical one when non-dimensional frequency was low. In the case that Biot number is 6.0 and 40, stresses of Numerical NSRD are higher than ones of theoretical NSRD, when non-dimensional frequency is in the range between 0.5 and 2.0. In this case, the inner surface temperature was approximately the same between numerical and theoretical ones, however, amplitude of theoretically calculated average temperature of the wall was larger than numerical one. When rearranging above results, theoretical NSRD can approximate and almost can bound numerical NSRD conservatively. When Biot number is 6.0 and 40, stresses of Numerical NSRD are higher than ones of theoretical NSRD within the error of 4.67 %. By adopting solution of temperature profiles of finite plates[7] instead of one of a semi-infinite solid, accuracy will be improved.

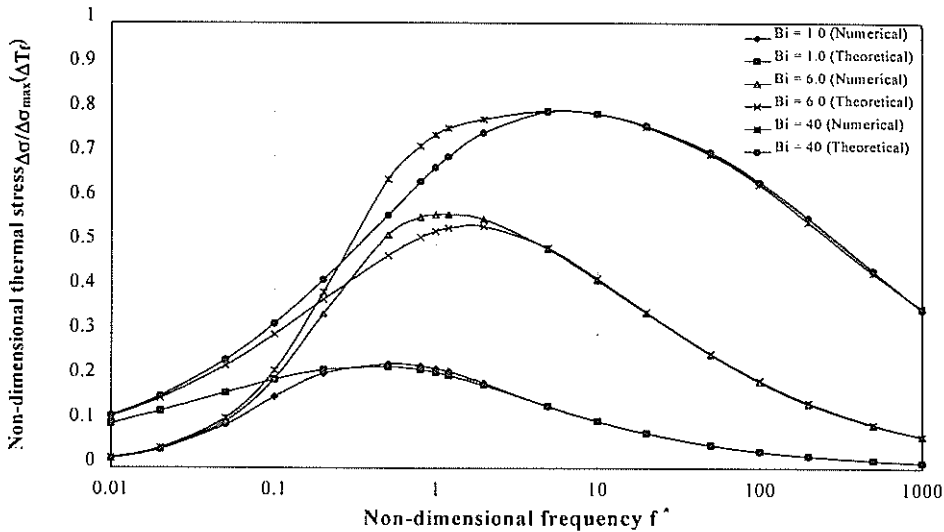


Fig.8 Comparisons of the numerical and the theoretical Non-dimensional structural response diagrams

**6. Conclusions**

Frequency response characteristics of structures to fluid temperature fluctuation and its mechanism were investigated by both numerical and theoretical methods. Consequently, it was clarified that induced stress amplitudes are attenuated by such factors which strongly depend on frequency as non-stationary heat transfer and thermal unloading. Based on this result, a structural response diagram

was derived, which can predict stress amplitude of structures from temperature amplitude and frequency of fluids. Furthermore, this diagram was generalized to be the non-dimensional structural response diagram (NSRD), by introducing non-dimensional parameters such as Biot number ( $Bi$ ), non-dimensional frequency ( $f^*$ ), and non-dimensional stress ( $\sigma^*$ ). Accuracy of NSRD was verified through comparison with F.F. calculated results.

The use of the NSRD appears to rationally evaluate thermal stress caused by thermal striping considering attenuation factors by both non-stationary heat transfer and thermal unloading. The NSRD can also give useful information on frequency range to which structural integrity is sensitive.

### **Acknowledgement**

The authors wish to express their gratitude to Mr. Ichiro Furuhashi of CRC Research Institute Inc. for several helpful discussions in the field of theoretical analysis. Thanks are due to participants of the IAEA coordinated research program on "Harmonization and Validation of Fast Reactor Thermomechanical and Thermohydraulic Codes and Relations Using Experimental Data", with whom we have discussed this problem.

### **References**

- [1] Muramatsu, T., 'Evaluation of Thermal Striping Phenomena at a Tee Junction of LMFR Piping System with Numerical Methods (1) Thermohydraulic Calculations, SMiRT15, Div.F (to be published)
- [2] Kasahara, N., 'Evaluation of Thermal Striping Phenomena at a Tee Junction of LMFR Piping System with Numerical Methods (2) Thermomechanical Calculations', SMiRT15, Div.F (to be published)
- [3] PNC, 'FINAS Version 12.0 User's Manual', PNC ZN9520 95-013, (1995)
- [4] Lejeail, Y., et al., 'A contribution to improvement of design rules on thermal striping', SMiRT14, Lyon, (1997)
- [5] Boley, B.A., 'Theory of Thermal Stresses', John Wiley & Sons, (1960)
- [6] Holman, J.P., "Heat Transfer", 7<sup>th</sup> ed., McGraw-Hill, (1990)
- [7] Norimatsu, S., et al., 'High-cycle non-steady thermal stress analysis – Thermal transient test on sodium components (X1)', PNC ZN941 77-57, In Japanese, (1977)